

Article

# Some Recent Results on High-Energy Proton Interactions

I. M. Dremin

Lebedev Physics Institute, 119991 Moscow, Russia; dremin@td.lpi.ru

Received: 6 December 2018; Accepted: 28 December 2018; Published: 3 January 2019



**Abstract:** Recent experimental results about the energy behavior of the total cross sections, the share of elastic and inelastic contributions to them, the peculiar shape of the differential cross section and our guesses about the behavior of real and imaginary parts of the elastic scattering amplitude are discussed. The unitarity condition relates elastic and inelastic processes. Therefore it is used in the impact-parameter space to get some information about the shape of the interaction region of colliding protons by exploiting new experimental data. The obtained results are described.

**Keywords:** proton; cross section; unitarity; spatial profile

---

## Foreword

*The paper is written in memory of my best friend Gariy Efimov. After graduating from Moscow Institute for Physics Engineering (MEPhI) in 1958 we worked on different but interrelated topics and kept common interests. He started working on quantum field theory and problems of the hadron structure. I got interested in models and phenomenology of high-energy particle interactions. Actually, particle interactions are determined by their structure. Recent studies clearly reveal this relationship. Here, I present the latest results about high-energy proton interactions which impress me and stay unexplained yet. I published several papers on them during latest years [1–6]. Unfortunately, I had no chance to discuss these results with my friend and to show new intriguing experimental figures reproduced in my reviews. Therefore I present them here with a hope they are of some interest for the reader.*

## 1. Introduction

Precise studies of particle interactions moved from cosmic rays to accelerator and collider data nowadays. Both elastic and inelastic processes are studied. There are numerous experimental results which are still waiting for their theoretical explanation. In spite of extreme successes of the strong interaction theory QCD (Quantum Chromodynamics) it happens still to be unable to describe many observational facts. Mathematical methods of QCD are yet not well enough developed to attack them directly.

The most widely used method in physics is the perturbative approach with its power series expansion using the smallness of the coupling constant. However it can be applied in QCD only to rather rare collisions with large transferred momenta (or masses) where the coupling strength becomes small due to the asymptotic freedom property, specific for QCD. It cannot be applied to main bulk of “soft” hadronic interactions with low transferred momenta because the coupling constant becomes large. Therefore several phenomenological approaches and ad-hoc assumptions have been attempted for description of experimental characteristics there and for getting reliable physical conclusions. Usually, many adjustable parameters have to be used for these models. Therefore their predictions become very flexible and less definite. In particular, the detailed spatial features of the hadron interaction region are not clearly established. To get them, more elaborate theoretical conclusions should be derived from

QCD about the energy and transverse momenta behavior of the amplitudes of particle interactions. Some (quite limited) help can be gained from the general principles of analyticity and unitarity of the scattering amplitudes.

The structure of the paper (my “would-be talk” to Gary) is as follows. First, general formulae are introduced. The corresponding new experimental data are described and briefly commented. They are used for getting some information about the spatial image of the proton interaction region. Final conclusions are presented at the very end.

## 2. New Data about the Elastic Scattering of High-Energy Protons

### 2.1. Some General Formulae

The experimental information about elastic scattering of protons is obtained from measurements of their differential cross sections  $d\sigma/dt(s, t)$  as functions of two Lorentz-invariant variables—the transferred momentum  $-t = 2p^2(1 - \cos\theta)$  at the scattering angle  $\theta$  and momentum  $p$  in the center-of-mass system and the total energy squared  $s = 4E^2 = 4(p^2 + m^2)$  where  $m$  denotes the proton mass. In what follows, it is convenient to use the scattering amplitude  $f(s, t)$  directly normalized to the value of the differential cross section such that

$$\frac{d\sigma}{dt} = |f(s, t)|^2 \equiv (\text{Re}f(s, t))^2 + (\text{Im}f(s, t))^2. \tag{1}$$

The dimension of  $f$  is  $\text{GeV}^{-2}$ . It must satisfy the general rigorous statement of the quantum field theory named the unitarity condition. The unitarity of the  $S$ -matrix  $SS^+ = 1$  relates the amplitude of elastic scattering  $f(s, t)$  to the amplitudes of inelastic processes  $M_n$  with  $n$  particles produced. In the  $s$ -channel they are subject to the integral relation (for more details see, e.g., [7,8]) which can be written symbolically as

$$\text{Im}f(s, t) = I_2(s, t) + g(s, t) = \int d\Phi_2 f f^* + \sum_n \int d\Phi_n M_n M_n^*. \tag{2}$$

The non-linear integral term represents the two-particle intermediate states of the incoming particles. The second term describes the shadowing contribution of inelastic processes to the imaginary part of the elastic scattering amplitude. Following [9] it is called the overlap function. This terminology is ascribed to it because it defines the overlap within the corresponding phase space  $d\Phi_n$  of the matrix element  $M_n$  of the  $n$ -th inelastic channel and its conjugated counterpart if one takes into account that the collision axis of initial particles must be deflected by an angle  $\theta$  for proton elastic scattering. It is positive at  $\theta = 0$  (no deflection!) but can change sign at  $\theta \neq 0$  due to the relative phases of inelastic matrix elements  $M_n$ 's.

At  $t = 0$  the relation (2) is known as the optical theorem

$$\text{Im}f(s, 0) = \sigma_{tot}/4\sqrt{\pi} \tag{3}$$

and leads to the general statement that the total cross section is the sum of cross sections of elastic and inelastic processes

$$\sigma_{tot} = \sigma_{el} + \sigma_{inel}, \tag{4}$$

i.e., that the total probability of all processes is equal to one.

The experimental data provide us the knowledge of the absolute value of the amplitude  $f$ . However, protons possess electric charges and the amplitude  $f$  should contain both nuclear and Coulomb terms. They become comparable and interfere at extremely low transferred momenta. Their interference helps to get some information about the real part of the nuclear amplitude at  $t \approx 0$  or about the ratio

$$\rho_0(s) = \frac{\text{Re}f(s, 0)}{\text{Im}f(s, 0)}, \tag{5}$$

where  $\text{Im}f(s, 0)$  is given by the optical theorem (3).

### 2.2. The Differential Cross Section

The differential cross section of elastic scattering of protons has a specific dependence on the transferred momentum  $t$  which evolves with energy  $s$  as measured by the collaboration TOTEM [10–12]. In Figures 1 and 2 it is shown for two energies of LHC.

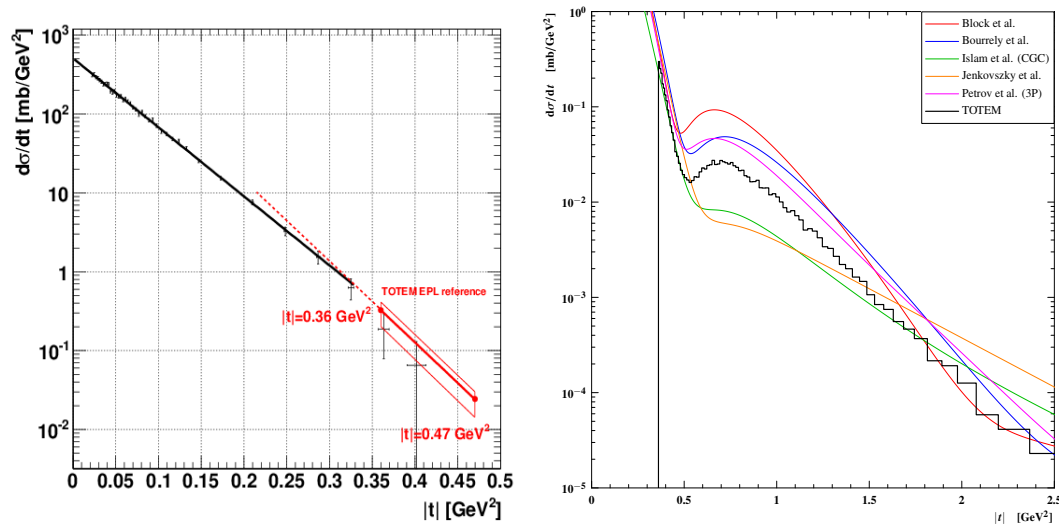


**Figure 1.** The differential cross section of elastic proton-proton scattering at the energy  $\sqrt{s} = 7$  TeV measured by the TOTEM collaboration. (Left) The region of the diffraction cone with the  $|t|$ -exponential decrease. (Right) The region beyond the diffraction peak. The predictions of five models are demonstrated. These Figures were reproduced in my review paper [1].

- Large amount of data (trigger rate  $50\times$  w.r.t. Run I)

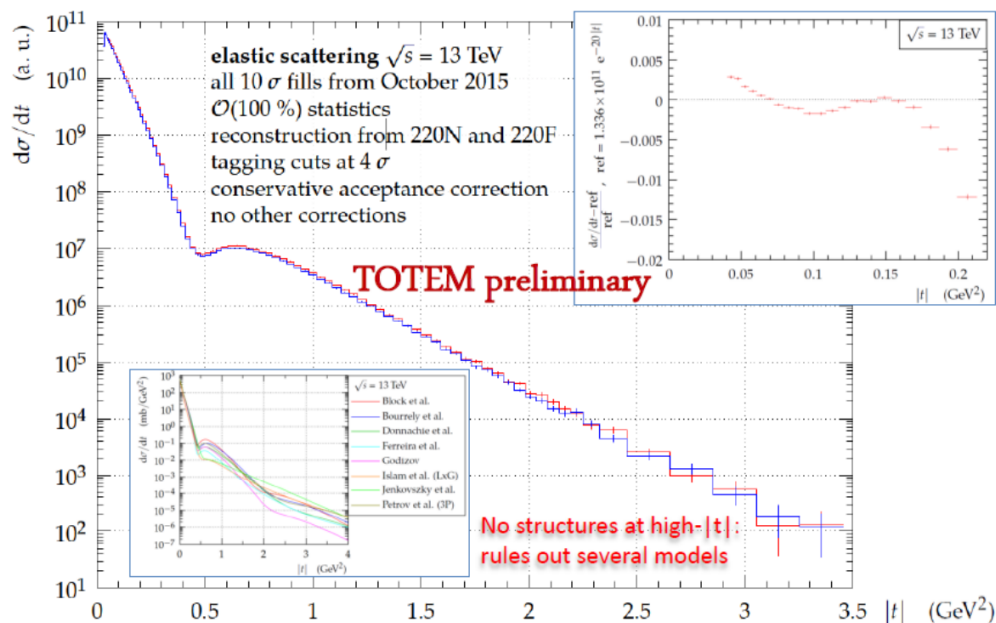


**Figure 2.** The differential cross section of elastic scattering of protons at 13 TeV reproduced in [5].

Let us discuss four regions which can be noticed in these Figures.

1. The region of extremely small transferred momenta near  $t = 0$  has been used for getting information about the real part of the nuclear amplitude as described above. The value of the ratio  $\rho_0$

was obtained in experiments at LHC energies to be about 0.1–0.14. These values are in agreement with earlier theoretical predictions [13,14] derived from dispersion relations using the analytical properties of the amplitude. At Intersecting Storage Rings (ISR) energies this ratio is very close to 0 both in experiment and theory. Therefore, it follows that the contribution of the real part to the differential cross section is very small (at the level less than 1%). Thus, the extrapolation of the differential cross section to  $t = 0$  determines the total cross section according to the optical theorem.

2. The second region of the diffraction peak at larger transferred momenta contributes mostly to the elastic cross section. It is characterized by approximately exponential decrease  $d\sigma/dt \propto \exp(Bt)$  up to the dip. The real part in near forward direction is small and should even diminish crossing 0 inside this region according to some reliable theoretical predictions [15]. Thus it can at most produce slight violations of the purely exponential fall-off attributed to the imaginary part. Theoretically it is described by the dominance of Regge-behavior with the slope  $B$  increasing as  $\ln s$  (due to  $s^{\alpha(t)}$ -behavior with linear Regge-trajectories  $\alpha(t) = \alpha_0 + \alpha't$ ). It is demonstrated in Figure 3 [16]. The shrinkage of the diffraction cone suggests that protons become larger at higher energies since  $B$  is proportional to the squared radius according to the Fourier transform.

3. The third region near the dip gives rise to the speculation that the imaginary part becomes 0 near the dip. The real part contributes to the differential cross section there. It is very small. The dip position moves to smaller transferred momenta at higher energies in accordance with the shrinkage of the diffraction cone.

4. Finally, the largest momenta measured at 13 TeV (from about  $0.7 \text{ GeV}^2$  to  $3.5 \text{ GeV}^2$ , see Figure 2) surprised us by demonstrating again the exponential decrease with about 4 times smaller slope than in the diffraction cone. At somewhat lower energies the so-called Orear regime dominated in there with slower  $\exp(-c\sqrt{|t|})$ -decrease [17,18]. It was interpreted as the byproduct of multiple rescattering on the same object. At 13 TeV the tail is damped stronger than the Orear regime and behaves analogously to the diffraction cone. That indicates now that some new internal structure (à la Rutherford finding!) of the twice smaller size enters the game. One can speculate that some smaller formations of quarks and gluons start playing the role there (diquarks, glueballs ...?).

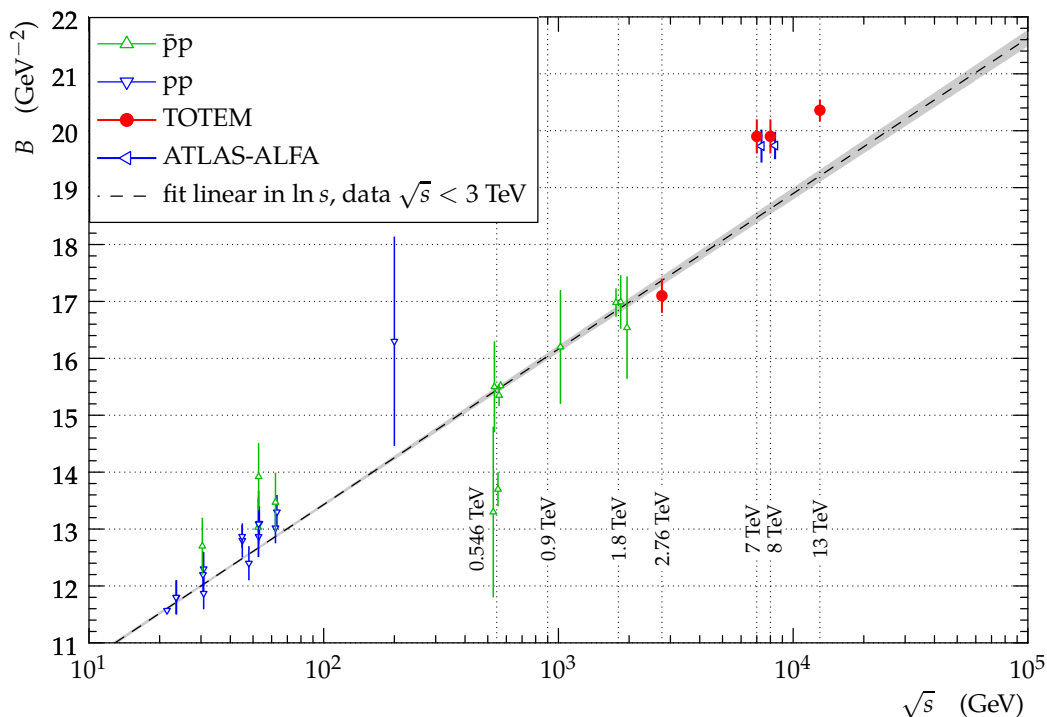
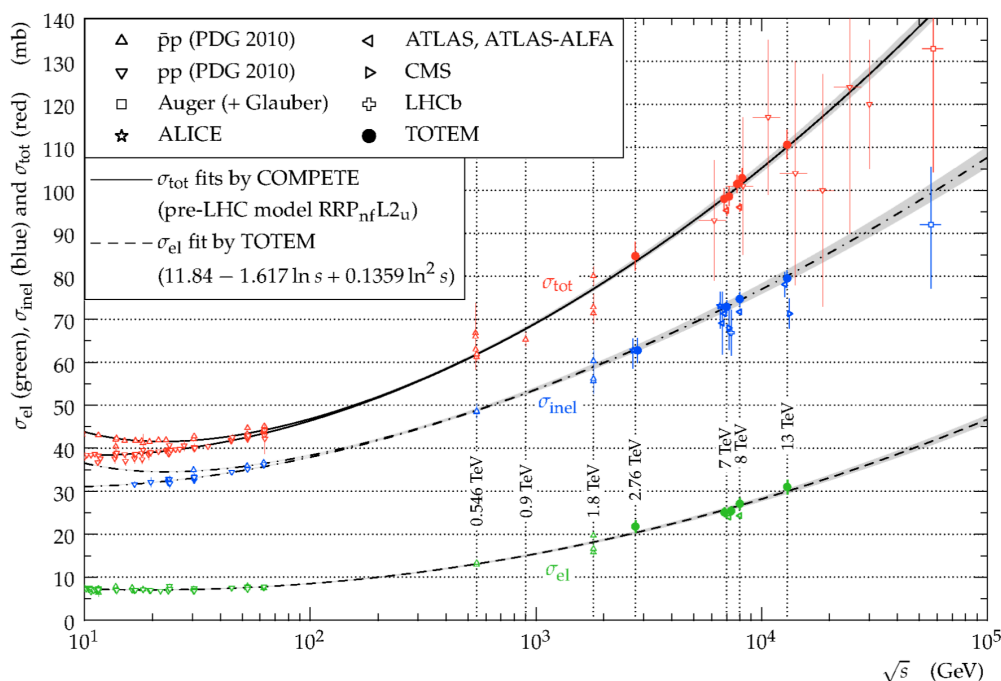


Figure 3. The energy dependence of the slope  $B$  of the diffraction cone reviewed in [5].

### 2.3. Energy Dependence of the Total, Elastic and Inelastic Cross Sections

The total cross section becomes known from extrapolation of the differential cross section to the optical theorem point  $t = 0$ . The integration of the differential cross section over all transferred momenta leads to the elastic cross section.

The physics results obtained at fixed-target accelerators dominated till 1970s. The proton-proton total cross section was steadily decreasing with energy increase. Theorists believed that at higher energies it will decrease further on either in a way similar to the cross section of the electron-positron annihilation or, at the best, tend asymptotically to some constant value somehow related to the proton sizes of the order of 1 fm. This belief was first strongly shattered in 1971 [19] by measurements at Serpukhov fixed-target accelerator (the available energy  $\sqrt{s}$  about 12 GeV in the center-of-mass system (c.m.s.)). The measured cross section of the interaction of positively charged kaons ( $K^+$ ) with protons started to increase slightly at energies from 8 to 12 GeV. At the very beginning this effect was not taken seriously enough. However soon it became well recognized at the ISR collider being confirmed by the rise of the total cross section of proton-proton collisions by about 10% in the wider energy range from about 10 to 62.5 GeV [20]. Nowadays much stronger effect is clearly seen at LHC up to 13 TeV as demonstrated in Figure 4 [16] for total, inelastic and elastic cross sections. The total cross section increases more than 2.5 times from ISR to LHC! Cosmic ray data are obtained by two collaborations Auger and Telescope Array. They also support this tendency up to higher energies almost 100 TeV even though with much less precision. Some of them are shown in Figure 4.



**Figure 4.** The energy dependence of the total, elastic and inelastic proton-proton cross sections reproduced in [5].

Such a behavior tells us that the size of the interaction region of protons becomes larger at higher energies. An upper bound on the increase of the total cross section was theoretically imposed when it was shown that it cannot increase more rapidly than as the logarithm of the energy to the second power (“Froissart-Martin bound”). However, it happens that the theoretical coefficient in front of the logarithm is very large. Therefore, phenomenologically, it does not exclude, at some interval of present energies, the use of a slow power-law energy dependence under this limit. Such a rise of hadronic cross sections is understood within scattering theory as being due to a virtual exchange of vacuum quantum numbers, known from Regge theory as a Pomeron. The power-like dependence can be ascribed to the

exchange of the so-called “supercritical Pomeron”, i.e., the pole singularity with intercept exceeding 1. The very existence of such Pomeron or other suitable Reggeon singularity as well as their dynamical origin are still unclear.

#### 2.4. Energy Dependence of the Ratio of Elastic to Total Cross Section

If the energy behavior of the total cross section can be phenomenologically interpreted in terms of Reggeon exchanges, the yet unsolved puzzle is provided by the completely unexpected energy dependence of the ratio of the elastic cross section to the total cross section. It is shown in Figure 5 [16] that this ratio is also increasing from ISR to LHC by more than 1.5 times. Probably, a more impressive way to express this is by the comparison of inelastic to elastic cross sections. The inelastic cross section is about 5 times larger than the elastic one at ISR while their ratio is less than 3 at LHC energies.

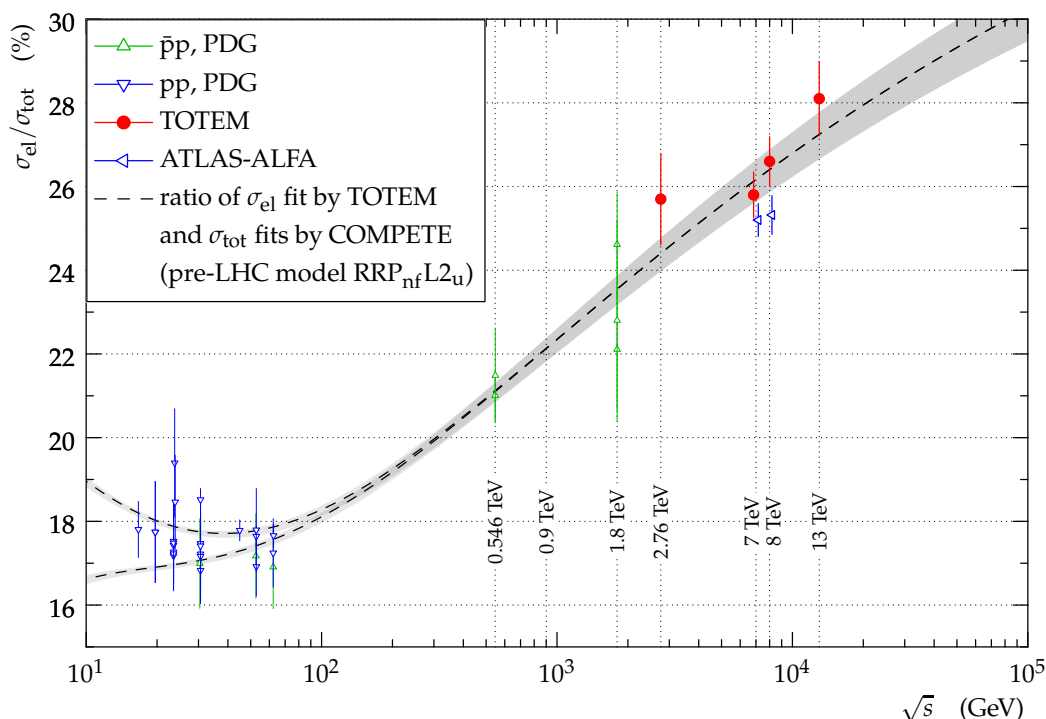


**Figure 5.** The energy dependence of the ratio of the elastic to total proton-proton cross sections (the survival probability) reproduced in [5].

The ordinate axis of Figure 5 tells us that the survival probability of protons to leave the interaction region intact is high enough and, what is more surprising, increases at higher energies. In other words, even being hit stronger, they do not break up producing secondary particles in inelastic collisions but try to preserve their entity. That contradicts our intuition based on classical prejudices. Naively, one could imagine the protons as two Lorentz-compressed bags colliding with high velocities. The bag model was widely used for describing the static properties of hadrons with quarks and gluons immersed in a confining shell. The color forces between the constituents are governed by QCD. Somehow Nature forbids the emission of colored objects (quarks and gluons) as free states because they never were observed in experiment. Thus these constituents can be created only in colorless combinations manifested in inelastic collisions as newly produced ordinary particles (mostly, pions) and resonances. The dynamics of internal fields during collisions and color neutralization is yet unclear. However the quantum origin of these fields must be responsible for the observed increase of the survival probability.

One could imagine the classical analogy to the bag model as a Kinder-surprise toy with many unseen pieces (quarks, gluons) hidden inside it. Their colorless blobs appear outside if two such toys

are broken in collision. These toys will never stay intact if hit strongly enough. Thus the increase of the survival probability of protons with increasing their collision energy is a purely quantum effect.

At the same time, one should keep in mind that this is a temporary effect because elastic cross section should never exceed the total one and their ratio must saturate asymptotically below 1.

### 3. The Spatial View of Interacting Protons

From earlier days of Yukawa prediction of pions, the spatial size of hadrons was ascribed to the pionic cloud surrounding their centers. The pion mass sets the scale of the size about  $1 \text{ fm} = 10^{-13} \text{ cm}$ . Numerous experiments using different methods confirmed this estimate with values of the proton radius ranging from 0.84 fm to 0.88 fm. This 5%-difference has been named as “proton radius puzzle”. Different methods used in various experiments could be in charge of this discrepancy. Their sensitivity to central and peripheral regions may be different. Among new experiments, it is worth mentioning recent results from the Jefferson laboratory [21] which reveal the internal gravitational forces inside the proton. It happens that they are repulsive at the center (up to 0.6–0.7 fm) and attractive (strongest at about 0.9 fm) at the periphery (“an extremely high outward-directed pressure from the center of the proton, and a much lower and more extended inward-directed pressure near the proton’s periphery”). It is interesting also that the lattice calculations [22] showed that “the gravitational strength” of a proton (its mass) is compiled only by 9% from the Higgs mechanism which provides the origin of quark masses. It is almost equally shared in three parts ( $30 \pm 5\%$ ) by kinetic energies of quarks and gluons and by their interactions. The three-quark content of protons is crucial for its static properties while the parton model is widely discussed for physics in collision. Surely, all these details of the proton substructure are important for their interaction.

Both central and peripheral regions play important roles in particle collisions. Traditionally, the hadron collisions were classified according to our prejudices about the hadron structure. The very external shell was considered to be formed by single pions as the easiest particle constituents. The deeper shells were constructed from heavier ( $2\pi, \rho$ -mesons etc.) objects. When treated in the quantum field theory terms, these objects contribute to the scattering amplitudes by their propagators which are damped down at the transferred momenta of the order of corresponding masses. According to the Heisenberg principle, the largest spatial extension is typical for the single pion exchange. That is why the one pion exchange model was first proposed in our early paper [23] for description of peripheral interactions of hadrons. It initiated the multiperipheral approach with exchange by a chain of pions. The very first and the simplest of them was the model of Amati et al [24] for pion-pion interactions with production of  $\rho$ -mesons. It predicted the cross section decreasing at high energies. That deficiency could be cured by creation of correlated groups of particles with larger masses (clusters) as described in the review papers [25–27]. Later, more central collisions with exchange of  $\rho$ -mesons and all other Regge particles were considered and included in the multiperipheral models of inelastic hadron interactions.

Meantime, the partonic description of inelastic processes with quarks and gluons playing the role of partons became well developed, in particular, for the electron-positron annihilation. Particle correlations were at the center of my studies of these processes [28] as well. Also, I speculated that massless gluons can be similar to photons and produce hadronic Cherenkov effect when they pass through the nuclear medium [29]. Then they can generate some specific correlations resulting in peculiar bumps of the angular distribution of produced particles similar to Cherenkov rings. Such bumps were observed in heavy-ion collisions. Alternative explanations were proposed also. Somewhat earlier, I got interested in the relation between elastic and inelastic processes imposed by the general principle of the quantum field theory called the unitarity condition (2). The elastic and inelastic processes are united in this condition by the statement that the total probability of them is equal 1. With its help, it happened to be possible to show [18,30] that some special behavior of the elastic scattering at large transferred momenta experimentally observed in some energy interval directly follows from this condition. From time to time, I discussed that with Gariy. Now I got again

interested in this approach as applied to the spatial view of proton collisions. After almost four years since he passed away, I describe in this paper the new experimental data and theoretical topics of 2015-2018 which we had no chance to discuss together [1,3,5,6].

### 3.1. The Unitarity Condition and the Spatial Image of Proton Interactions

The space structure of the interaction region of colliding protons can be studied by using information about their elastic scattering with the help of the unitarity condition. For that purpose, the relation (2) must be transformed to the space representation. The whole procedure becomes simplified because in the space representation one gets an algebraic relation between the elastic and inelastic contributions to the unitarity condition in place of the more complicated non-linear integral term  $I_2$  in Equation (2).

The Fourier transformation which is at the origin of the Heisenberg principle relating space-time to energy-momentum characteristics leads to the power-like dependences if applied directly to the propagators. However, the exponential fall-off is more typical for the general functional behavior of hadronic interactions as seen, for example, from the shape of the diffraction cone of their elastic scattering differential cross section. Therefore, one has to cure this deficiency and ascribe the exponents to the Regge type behavior of vertex functions. Thus the propagators lose their heuristic role leaving it to the phenomenological prescriptions. The simple spatial view is lost as well. To get back the direct insight to it one has to deal with the impact-parameter representation of the scattering amplitude. Its connection with experimental results on the transferred momentum dependence is established by the Fourier–Bessel transformation. The traditional prejudice is that the large impact parameters contribute mostly to the cross section at small transferred momenta. However, even though the exponential shape of the Fourier transform favors that, this statement depends strongly on the shape of the amplitude itself in the impact-parameter presentation.

It would be desirable to get some information about inelastic processes not from phenomenological models but from more general principles. At first glance, this way could be provided by one of them—the general unitarity condition relates directly elastic and inelastic amplitudes. The properties of elastic processes have been studied experimentally rather precisely. Using them, one can hope to learn some features of inelastic processes. This proposal leads to interesting results but requires additional assumptions discussed below in detail.

To define the geometry of the collision we must express all characteristics presented by the angle  $\theta$  and the transferred momentum  $t$  in terms of the transverse distance between the trajectories of the centers of the colliding protons—namely the impact parameter,  $b$ . This is easily carried out using the Fourier–Bessel transform of the amplitude  $f$ . It retranslates the experimentally available momentum data to the corresponding transverse space features. The result is written as

$$i\Gamma(s, b) = \frac{1}{2\sqrt{\pi}} \int_0^\infty d|t| f(s, t) J_0(b\sqrt{|t|}) \tag{6}$$

where  $J_0$  is the Bessel function of 0-th order.

The unitarity condition (2) expressed in the  $b$ -representation reads

$$G(s, b) = 2\text{Re}\Gamma(s, b) - |\Gamma(s, b)|^2. \tag{7}$$

Thus some information about inelastic processes  $G(s, b)$  can be gained just from the elastic scattering amplitude  $f$  using Equations (6) and (7). The left-hand side (the overlap function in the  $b$ -representation) describes the transverse impact-parameter profile of inelastic collisions of protons. It is just the Fourier–Bessel transform of the overlap function  $g$ .

It is necessary to stress from the very beginning that the main difficulty in getting any information about  $G(s, b)$  is in calculation of  $\Gamma(s, b)$  which requires knowledge of both real and imaginary parts of  $f$  at all transferred momenta  $t$  for a given energy  $s$ .

The integral contribution of the real part of the amplitude  $f$  to the unitarity condition should be small (see estimates in Ref. [2] and Figures 6 and 7 below) and is neglected in what follows. Then the unitarity condition is written as

$$G(s, b) = \zeta(s, b)(2 - \zeta(s, b)) = \text{Re}\Gamma(s, b)(2 - \text{Re}\Gamma(s, b)). \tag{8}$$

Thus, according to Equation (8), the shape of  $G(s, b)$  is determined by the integral contribution over all transferred momenta from the imaginary part of the elastic amplitude. The sign of  $\text{Im}f$  cannot be determined from  $d\sigma/dt$ .

The absolute maximum of  $G(s, b)$  is reached if  $\text{Re}\Gamma(s, b)=1$ . At ISR energies the maximum value at  $b = 0$  is less than 1, especially at lower energies of ISR [31] (see Figure 6 [32]). It becomes close to 1 at 7 TeV.

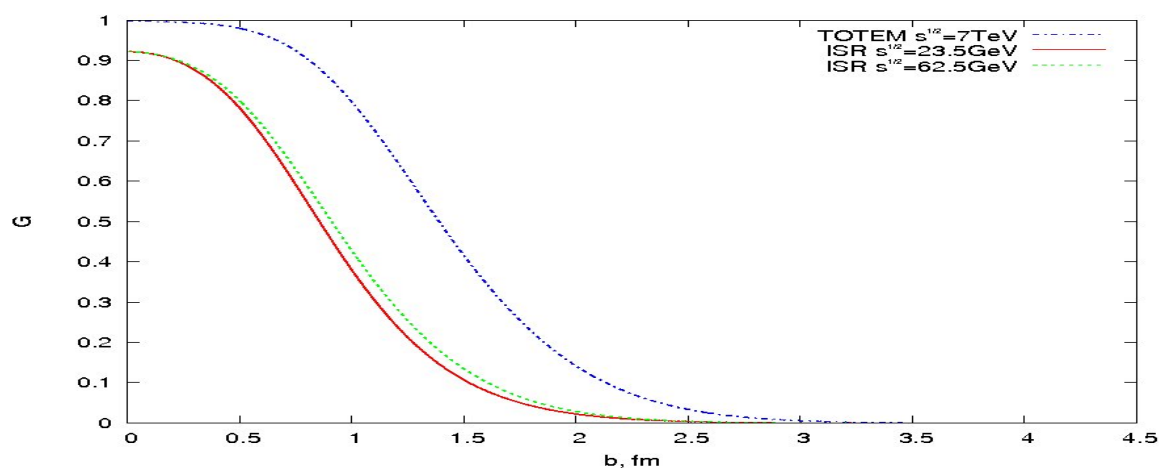


Figure 6. The proton profile  $G(s, b)$  at 7 TeV (upper curve) compared to those at ISR energies 23.5 GeV and 62.5 GeV (the interpolation procedure of experimental data has been used) shown in [1].

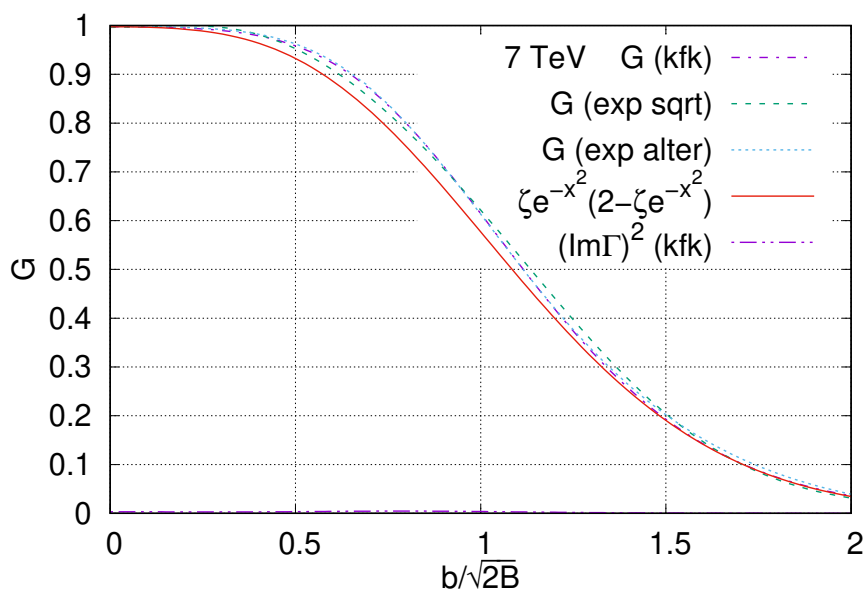


Figure 7. The transverse impact-parameter profile ( $G$ ) of inelastic collisions of protons at 7 TeV in different assumptions: kfk-model (dash-dotted line),  $\text{Im}f(s, t) = \sqrt{d\sigma/dt}$  calculated from experimental data (dash line),  $\text{Im}f(s, t) = \sqrt{d\sigma/dt}$  inside the diffraction cone and  $\text{Im}f(s, t) = -\sqrt{d\sigma/dt}$  outside cone also calculated from experimental data (dotted line), shape  $\zeta \exp(-x^2)(2 - \zeta \exp(-x^2))$  with  $\zeta = 0.95058$  (solid line). Also the square of the imaginary part of  $\Gamma$  for kfk-model is shown by dash-double-dot line (very small contribution of the real part of the amplitude!).

### 3.2. Shapes of the Interaction Region

Let us compare two extreme assumptions about  $\text{Im}f(s, t)$ :

(1) it is given either by  $+\sqrt{d\sigma/dt}$  at all  $t$  or

(2) it is positive inside the cone and negative  $-\sqrt{d\sigma/dt}$  outside it (at  $|t| > |t_0|$ , where  $t_0$  is the minimum position).

The shapes of the interaction region have been computed for these two assumptions with spline interpolation of experimental data for  $d\sigma/dt$  used. They are shown in Figures 7 and 8 for 7 and 13 TeV. The region of small impact parameters is enlarged in Figure 9 because the most intriguing difference between various assumptions is seen just there.

It is clearly seen in Figure 9 that the assumption about the everywhere positive imaginary part leads to the dip  $G(s, 0) < 1$  for central collisions at  $b = 0$  (easily noticed at 13 TeV). The maximum  $G(s, b_{max}) = 1$  moves to  $b_{max} > 0$ , i.e., the toroid-like shape is formed. The possibility of dip at  $b = 0$  was first considered in Ref. [33]. If the imaginary part becomes negative at large transferred momenta, no dip appears and the BEL-shape is recovered.

Thus one concludes that the assumption about the positivity of the imaginary part of the amplitude at all available  $t$ -values leads to the validity of the earlier speculation about the toroidal shape of the interaction region (see the review paper [3]). In particular, this conclusion was supported if the purely exponential shape of the imaginary part in the diffraction cone with experimental values for its slope  $B$  was extended to all transferred momenta [34,35] in place of using its experimental form at large  $|t|$ . Then the positive exponential tail of the elastic amplitude with rather large slope  $B/2$  provides the slight dip at  $b = 0$ . Albeit it is much smaller than for our first variant due to the lower tail and is hard to resolve at the scale of Figures 7 and 8 where it is shown as  $\zeta \exp(-x^2)(2 - \zeta \exp(-x^2))$ . Analytically, for that case, the shrinkage of the diffraction cone at high energies (the energy increase of the slope  $B$ ) is directly related to the energy increase of the ratio of elastic to total cross section ( $B \approx \sigma_{el}/16\pi\sigma_{tot}^2$ ), which, in its turn, determines the dip at  $b = 0$  if  $\sigma_{el}/\sigma_{tot} > 0.25$  as it happens at 13 TeV.

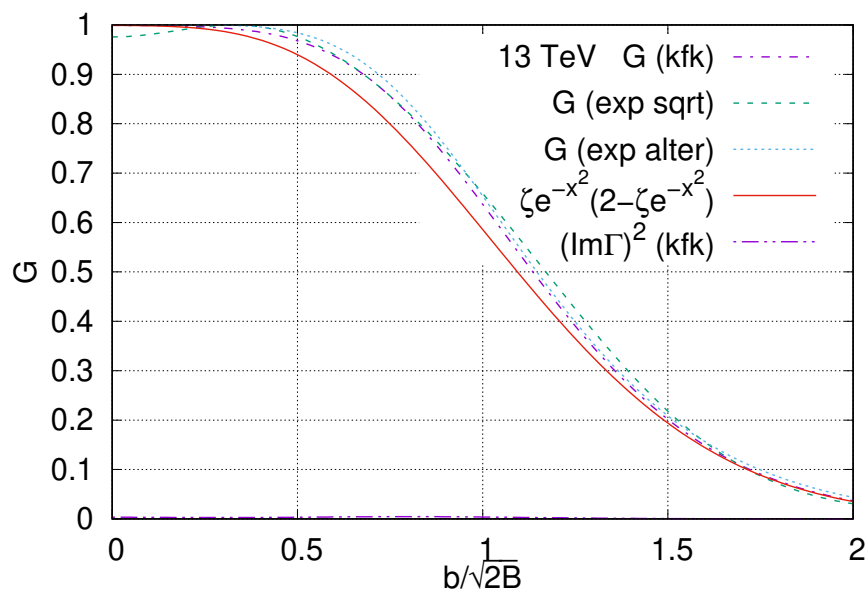
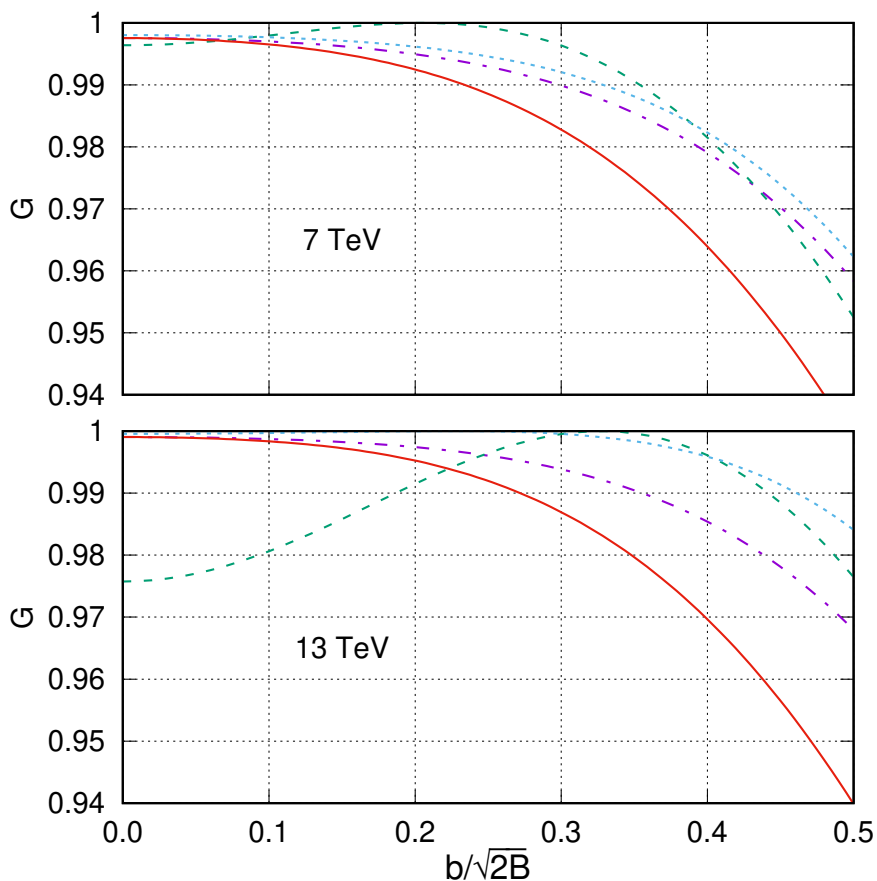


Figure 8. The same as Figure 7 but at 13 TeV and with  $\zeta = 0.96906$ .



**Figure 9.** The area near  $b = 0$  of Figures 7 and 8 in more details.

Another shape of the interaction region of the BEL-type follows from the so-called kfk-model [36]. This phenomenological model exploits some QCD inspired ideas and predicts both real and imaginary parts of the amplitude using numerous parameters derived from precise fits of measured cross sections. According to it, the real part becomes zero inside the diffraction cone region while the imaginary part possesses zero near the minimum of the differential cross section (it is seen in Figure 1). Its value at the minimum is filled by a small negative real part. The imaginary part becomes also negative at larger transferred momenta. It reminds the second variant. Therefore  $G(s, b)$  has no dip at the center  $b = 0$ . It is also demonstrated in Figures 7 and 8. Some analysis of the kfk-model showing its “anatomy” was done in Ref. [2]. It is possible to verify our assumption about the smallness of the real part of the amplitude for this model. The real part of the amplitude has been computed at 7 and 13 TeV. Its contribution to the shape of  $G(s, b)$  in Equation (7) happens to be extremely small (within the limits of experimental accuracy) and can be neglected (see Figure 8). The model predicts the BEL-shape of the interaction region even at asymptotically high energies.

It would be interesting to confront its prediction with new results obtainable with the help of the Levy-interpolation method [37] by which both the real and imaginary parts of the amplitude can be found out. The model of Ref. [36] proposes the definite form of the elastic scattering amplitude inspired by QCD ideas. Its parameters are fitted by the existing experimental data and used for extrapolation to higher energies. At its turn, the Levy-approach [37] is aimed on the direct interpolation of the differential cross section by the complete orthonormal set of complex functions suited for exponential and power-like dependence on transferred momenta revealed in experiment. The comparison of the results obtained in these two approaches on their predictions for the dip at  $b = 0$  would be very instructive.

Quite special feature of  $G(s, b)$  at ISR energies was noticed in [31] where genuine experimental data were used. At its tail of large impact parameters from 2 fm to 2.5 fm a slight bump was observed. No bump was obtained in [38] where some interpolation of the data was used. The results in Figures 7 and 8 do not show any indication on such a bump. The corresponding values of  $b = 2\sqrt{2B} \approx 2.5$  fm are similar to those in [31].

#### 4. Conclusions

As described above, numerous new experimental data lead to many new puzzles. Among them the problem of the spatial view of protons asks for some additional information.

According to Equations (6) and (7), the spatial shape of the proton interaction region is determined by the integrals of the elastic scattering amplitude over all transferred momenta. The knowledge of its modulus obtainable from measurable differential cross sections is not enough to compute them. The prescription  $\text{Im}f \approx |f| \approx +\sqrt{d\sigma/dt}$  leads to the toroidal shape at the highest LHC energies. In contrast, the negative values of  $\text{Im}f$  at large transferred momenta recover the BEL-regime.

Thus, the problem of the spatial shape of the proton interaction region cannot be solved rigorously unless the behavior (and, especially, the sign of the imaginary part!) of the elastic scattering amplitude is known. Unfortunately, there seem to be no ways to get precise experimental or theoretical information about it now. Therefore, one has to rely on “reasonable” speculations and phenomenological models confronted with a wide spectrum of experimental data.

**Funding:** This research received no external funding.

**Conflicts of Interest:** The author declares no conflict of interest.

#### References

1. Dremin, I.M. Interaction region of high energy protons. *Phys.-Uspekhi* **2015**, *58*, 61. [CrossRef]
2. Dremin, I.M.; Nechitailo, V.A.; White, S.N. Central and peripheral interactions of hadrons. *Eur. Phys. J. C* **2017**, *77*, 910. [CrossRef]
3. Dremin, I.M. Unexpected interaction properties between high energy protons. *Phys.-Uspekhi* **2017**, *60*, 333. [CrossRef]
4. Dremin, I.M. Several effects unexplained by QCD. *Universe* **2018**, *4*, 65. [CrossRef]
5. Dremin, I.M. Some new discoveries at colliders. *Phys.-Uspekhi* **2018**, *61*, 381. [CrossRef]
6. Dremin, I.M.; Nechitailo, V.A. Inelastic profiles of protons at 7 and 13 TeV. *Eur. Phys. J. C* **2018**, *78*, 910. [CrossRef]
7. PDG Group. Review of particle physics. *China Phys. C* **2014**, *38*, 090513. [CrossRef]
8. Dremin, I.M. Elastic scattering of hadrons. *Phys.-Uspekhi* **2013**, *56*, 3. [CrossRef]
9. Van Hove, L. A phenomenological discussion of inelastic collisions at high energies. *Nuovo Cimento* **1963**, *28*, 798. [CrossRef]
10. Antchev, G.; D’Orazio, A.; Barrera, C.B. Luminosity-independent measurement of the proton-proton total cross section at  $\sqrt{s} = 8$  TeV. *Phys. Rev. Lett.* **2013**, *111*, 012001. [CrossRef]
11. Antchev, G.; D’Orazio, A.; Barrera, C.B. Evidence for non-exponential elastic proton-proton differential cross-section at low  $|t|$  and  $\sqrt{s} = 8$  TeV by TOTEM. *Nucl. Phys. B* **2015**, *899*, 527. [CrossRef]
12. Csörgö, T. Talk at Low-x 2017, 12–18 June 2017. Biscegli. Available online: <https://indico.cern.ch/event/609299/> (accessed on 1 January 2019).
13. Dremin, I.M.; Nazirov, M.T. Real part of the forward elastic scattering amplitude and high-energy behavior of the total cross sections. *JETP Lett.* **1983**, *37*, 198.
14. Block, M.M.; Gregores E.M.; Halzen F.; Pancheri, G. Measurements of the rising photon-photon total cross section at the CERN LEP. *Phys. Rev. D* **1998**, *58*, 017503. [CrossRef]
15. Martin, A. Asymptotic behaviour of the real part of the scattering amplitude at  $t \neq 0$ . *Lett. Nuovo Cimento* **1973**, *7*, 811. [CrossRef]

16. Antchev, G.; D’Orazio, A.; Barrera, C.B.; Burkhardt, H.; Stefanovitch, R.; Grzanka, L.; Kopal, J.; Sziklai, J.; Catanesi, M.G.; Royon, C.; et al. First measurement of elastic, inelastic and total cross-section at  $\sqrt{s} = 13$  TeV by TOTEM and overview of cross-section data at LHC energies. *arXiv* **2017**, arXiv:1712.06153.
17. Orear, J. Transverse Momentum Distribution of Protons in pp Elastic Scattering. *Phys. Rev. Lett.* **1964**, *12*, 112. [[CrossRef](#)]
18. Andreev, I.V.; Dremin, I.M. Large-angle Elastic Scattering. *JETP Lett.* **1967**, *6*, 262.
19. Denisov, S.P.; Donskov, S.V.; Gorin, Y.P. Total cross sections of  $\pi^+$ ,  $K^+$  and p on protons and deuterons in the momentum range 15–60 GeV/c. *Phys. Lett. B* **1971**, *36*, 415–421. [[CrossRef](#)]
20. Amaldi, U. *40th Anniversary of the First Proton-Proton Collisions in the CERN Intersecting Storage Rings (ISR), Colloquium, 18 January 2011*; (CERN-2012-004); CERN: Geneva, Switzerland, 2012.
21. Burkert, V.D.; Elouadrhiri, L.; Girod, F.X. The pressure distribution inside the proton. *Nature* **2018**, *557*, 396. [[CrossRef](#)]
22. Yang, Y.-B.; Liang, J.; Bi, Yu.-J.; Chen, Y.; Draper, T.; Liu, K.-F.; Liu, Z. Proton Mass Decomposition from the QCD Energy Momentum Tensor. *Phys. Rev. Lett.* **2018**, *121*, 212001. [[CrossRef](#)]
23. Dremin, I.M.; Chernavsky, D.S. Peripheral interactions of nucleons at 9-BeV. *JETP* **1960**, *38*, 229.
24. Amati, D.; Stanghellini, A.; Fubini, S. Theory of high-energy scattering and multiple production. *Nuovo Cimento* **1962**, *26*, 896. [[CrossRef](#)]
25. Dremin, I.M.; Dunaevsky, A.M. The multiperipheral cluster theory and its comparison with experiment. *Phys. Rep.* **1975**, *18*, 159. [[CrossRef](#)]
26. Dremin, I.M.; Quigg, C. The Cluster Concept in Multiple Hadron Production. *Science* **1978**, *199*, 937. [[CrossRef](#)] [[PubMed](#)]
27. DeWolf, E.; Dremin, I.M.; Kittel, W. Scaling laws for density correlations and fluctuations in multiparticle dynamics. *Phys. Rep.* **1996**, *270*, 1. [[CrossRef](#)]
28. Dremin, I.M.; Gary, J.W. Hadron multiplicities. *Phys. Rep.* **2001**, *349*, 301. [[CrossRef](#)]
29. Dremin, I.M. Coherent hadron radiation at extremely high energies. *JETP Lett.* **1979**, *30*, 140.
30. Andreev, I.V.; Dremin, I.M.; Gramenitskii, I.M. High-energy pp large-angle scattering. *Nucl. Phys.* **1969**, *10*, 137. [[CrossRef](#)]
31. Amaldi, U.; Schubert, K.R. Impact parameter interpretation of proton-proton scattering from a critical review of all ISR data. *Nucl. Phys. B* **1980**, *166*, 301. [[CrossRef](#)]
32. Dremin, I.M.; Nechitailo, V.A. Proton periphery activated by multiparticle dynamics. *Nucl. Phys. A* **2013**, *916*, 241. [[CrossRef](#)]
33. Troshin, S.M.; Tyurin, N.E. Beyond the black disk limit. *Phys. Lett. B* **1993**, *316*, 175. [[CrossRef](#)]
34. Dremin, I.M.; White, S.N. The Interaction Region of High Energy Protons. *arXiv* **2016**, arXiv:1604.03469.
35. White, S.N. Talk at the Conference QCD at Cosmic Energies, Chalkida, Greece, May 2016. Available online: <http://www.lpth.jussieu.fr/cosmic2016/TALKS/White.pdf> (accessed on 1 January 2019).
36. Kohara, A.K.; Ferreira, E.; Kodama, T. pp elastic scattering at LHC energies. *Eur. Phys. J. C* **2014**, *74*, 3175. [[CrossRef](#)]
37. Csörgö, T.; Pasechnik, R.; Ster, A. Odderon and proton substructure from a model-independent Levy imaging of elastic pp and p $\bar{p}$  collisions. *arXiv* **2018**, arXiv:1807.02897.
38. Henzi, R.; Valin, P. Towards a blacker, edgier and larger proton. *Phys. Lett. B* **1983**, *132*, 443. [[CrossRef](#)]

